

Deliverable Task 1.1
Part B

University of Stuttgart

Simulations on Use Cases for the Usage
of Flexibilities in Distribution Grids



CALLIA – Open Inter-DSO Electricity Markets for RES Integration

funded under the ERA-Net Smart Grids + scheme of the European Commission

Document Information

Contract Number	77616
Project Website	www.callia.info/en/
Authors	Daniel Contreras, Krzysztof Rudion (University of Stuttgart, IEH, Germany)
Reviewer	Janhavi Devarajan (Stadtwerke Heidelberg Netze, Germany)
Keywords	Use of Flexibilities, Use Cases, Flexibility Market

Change Log

Version	Description of Change	Date
0.0	First draft	30/04/2018
1.0	Version ready for review	28/06/2018
2.0	Version ready to publish	09/07/2018

Summary

Task 1.1 is the initial task of CALLIA and its definitions and results will influence the development of the project. The objectives of the task can be divided in two main sections, the first being the definition of local balancing challenges and opportunities, and the second being the definition of new products, services and approaches related to intra-DSO and inter-DSO balancing and trading depending on section 1. The definition of the use cases to be researched within CALLIA will be defined by the involved grid operators based problems faced by DSOs with respect to the integration of DER in the distribution grids.

The second section of the task involves the simulation based analysis of the potential of local balancing and intra-DSO and inter-DSO exchange. Parts of distribution grids of the involved grid operators will be modelled and these will allow for the simulation of the use cases defined initially . In order to reduce computation times and optimize resources, ways to aggregate the information and parts of the grid have to be defined. The number of modelled nodes will be reduced by means of aggregation of underlying grids to a connection point. Additionally, the grid models will allow the grid operators to identify the best suitable sections of their distribution grids, to be used for the pilot field tests later in WP 3.

The grid models and simulations will allow the generation of flexibility estimation maps at some distribution grid connection nodes (e.g. DSO/TSO transformers), which will help evaluate how much Flexibility can a section of the grid provide, taking into consideration also the probabilistic aspects of the generation and load profiles. The defined products and services will be tested within these simulations. Additionally, the grid operators will select part of their grids that could be suitable for the implementation of the field tests later in the project.

The results of Task 1.1 will work in parallel and very close to Task 1.2 (Business Cases) and Task 1.3 (Regulatory Frame); its outputs will serve as input for Task 2.1 (CALLIA architecture), Task 2.3 (Trading Information), Task 2.4 (device and platform agents), Task 2.5 (Market Plat-form), Task 3.1 (HiL simulations) and Task 3.2 (Preparation of Field Tests).

Contents

Summary	2
List of Abbreviations and Acronyms	4
1. Introduction	5
2. Use of Flexibilities for the Provision of Ancillary Services	7
2.1 Flexibility Providing Units (FPU)	7
2.2 Linear Modelling of FPUs	8
3. Aggregation Model for Flexibilities	9
3.1 Linear flexibility aggregation methodology	10
3.2 Linear Optimal Power Flow Equations	11
3.3 Flexibility Aggregation Method	14
3.4 Flexibility Aggregation over Different Voltage Levels	16
<i>Step 1: Aggregation of Single LV Grids</i>	17
<i>Step 2: Aggregation of MV Distribution Grid</i>	17
4. Case Study for Callia	18
4.1 Grid Model Definition	18
4.2 Flexibility Aggregation	19
4.3 Callia Use Cases	22
a. Congestion Management	22
b. Local Balancing	24
c. Grid Losses Mitigation	25
d. Voltage Control	27
5. Conclusions	28
Bibliography	30

List of Abbreviations and Acronyms

Acronym	Meaning
BRP	Balance Responsible Party
CHP	Combined Heat Power
DER	Distributed Energy Resources
DSM	Demand Side Management
DSO	Distribution System Operator
FPU	Flexibility Providing Unit
HV	High Voltage
kW	Kilo-Watt
LV	Low Voltage
MV	Medium Voltage
MVA	Mega-Volt-Ampere
MVA _r	Mega-Volt-Ampere-reactive
MW	Mega-Watt
NR-PF	Newton-Raphson Power Flow
OLTC	On Load Tap Changer
OPF	Optimal Power Flow
PV	Photovoltaic
RES	Renewable Energy Source
TSO	Transmission System Operator
WP	Work Package

1. Introduction

Increased penetration of distributed energy resources (DER), i.e. renewable energies, storage systems, electric vehicles, among others, is forcing distribution grid operators (DSO) to change the way their grids need to be operated [1]. Some of the challenges that DSOs are facing have been described in [2]; where the rise of congestions at the distribution level, as well as the maintenance of the power quality of the grid are among them. The potential use of flexibilities provided as ancillary services to the grid to solve some of the issues raised in [2], have been defined in the Deliverable 1.1 Part A of the Callia project.

The concept of flexibility may have different definitions, as was reviewed in [3]. In this case, flexibility is defined as the “modification of generation or consumption in reaction to an external signal”, extended to reactive power as well [2]. Within the Callia project, a market platform where grid operators can reach for flexibilities will be developed. In order to make such a market platform effective, the communication and coordination between grid operators (especially between DSO-DSO and DSO-TSO) needs to be improved, as stated in [4]. One example is Germany, where each TSO supplies more than one hundred DSOs within its control zone. This scenario makes it very difficult for any of the TSOs to achieve a proper level of coordination with all of their corresponding DSOs. Therefore, the improvement of the TSO-DSO coordination acquires great relevance. Within the SmartNet project, different coordination schemes between TSO and DSO were identified and studied [5].

In order to help with the coordination between grid operators, new methods to exchange data and information need to be developed. Within the frame of the EvolvDSO project, such a method was initially developed, where the flexibility provision of a distribution grid is represented in an aggregated way at the DSO-TSO interconnection point, through a convex polygon [6]. In a first attempt to introduce the model, an approach based on Monte Carlo simulations was studied in [7]. The method performs thousands of load flow calculations on a grid model considering multiple configuration of set points of a conglomerate of flexible resources (generators, loads, OLTC transformers, etc.). The same authors have proposed in [6] and [8], an improvement to this method in the form of a non-linear mixed-integer optimization problem, called the Interval Constrained Power Flow (ICPF) algorithm. A variation of this algorithm is presented in [9], where an alternative way to explore the flexibility range is proposed.

In this deliverable, an adaptation of the concept introduced in [8] is presented, where the optimization problem is linearized, in order to increase the speed of the calculation. The objective is to be able to assess the flexibility of large grid models with several flexibility providing units (FPU) connected to them. This aggregation algorithm is performed in multiple steps in the case of distribution grids with different voltage levels. The use cases defined in the Deliverable 1.1 - Part A are evaluated in a simulation environment. The objective is to appraise the effectiveness of the usage of flexibilities for the proposed use cases, including congestion management issues, voltage issues and the concept of loss mitigation. The concept of local balancing is considered for all approaches.

First, a definition of flexibilities is given, which is the base for the simulations. Then the case study is presented, where an abstraction of a real grid in the city of Heidelberg in Germany is used as a model to compare the use cases. Consequently, the use cases are simulated considering typical days and situations in this grid. Finally, the results are analyzed.

The document is divided into three parts: first, in Chapter 2, the usage of flexibilities for the provision of ancillary services is discussed, while introducing a set of linear models representing the technical limitations of typical flexible distribution grid resources. In Chapter 3, an aggregation algorithm for flexibilities based on linear programming is introduced. Finally, in Chapter 4 a case study for the evaluation of the proposed algorithm is presented, among simulations of the use cases for flexibilities defined in the Deliverable 1.1 - Part A of the Callia Project. The document closes with the conclusions from the performed simulations and their impact on the following steps of the Callia Project.

2. Use of Flexibilities for the Provision of Ancillary Services

2.1 Flexibility Providing Units (FPU)

Any decentralized generating unit, storage system or controllable load could be considered as a flexibility provider. For this, the device need to be remotely controllable, where the operation point can be modified through an external signal. Within the Callia framework, this signal should be provided by a market platform. Here, the concept of FPU is applied to refer every kind of controllable grid utility, taking the control of both active, and reactive power into consideration. A review on FPUs that can be found in power grids at different voltage levels is provided here:

- **Photovoltaic Generation (PV):** The integration of PV generation has seen a very large increase in MV and LV grids. The modules are connected to the grid through power inverters, which allow the adjustment of the provision of active power and in some cases reactive power as well. For example, newer PV generators in Germany are required to adapt their power factor up to 0.9 to provide voltage support to the grid . Although the power generation of PV is always defined by the local solar radiation, the power supply of the PV panel could be curtailed in order to allow the provision of positive active power flexibility, as well as negative flexibility [10] [11].
- **Wind Generation (WG):** Wind generators with doubly fed induction generators (DFIG) can control active and reactive power independently within a certain range, bounded by the technical limitations of the asynchronous electrical machine. Wind generators with full-inverters allow an entirely independent control of active and reactive power, bounded by the limits of the inverter. In both cases, maximum generation depends on local wind speed, but use cases for the deloaded operation of such generators have been investigated, especially for frequency control purposes. Many control techniques have been developed, that allow the regulation of the active and reactive power output, depending on the use case [12].
- **Controllable Loads:** Demand side management (DSM) has focused primarily on the control of active power consumption of industrial loads. With the penetration of intelligent devices in the households, i.e. washing machines or controllable LED illumination, DSM is increasing its interest in controlling these kinds of smaller loads as well. Every customer has his own consumption pattern, which changes from house to house and between commercial, industrial and residential customers. So far, specific $\cos(\varphi)$ limits are expected to be maintained by each customer, especially for commercial and industrial customers, in some cases subjected to penalties. For households, traditionally, a fixed $\cos(\varphi)$ is considered during grid planning simulations, due to the lack of measurements. In the case of industrial loads, typically reactive power compensation at the connection point to the grid is required, providing a fixed $\cos(\varphi)$ to the eyes of the grid. This can be represented as a linear relation of active and reactive power through [13].
- **Synchronous Generators (SG):** Large power plants, powered by water, coal, gas or radioactive material, all contain synchronous generators, which allow the regulation of active and reactive power supply. This can be performed mechanically, by controlling the primary energy supply, or by controlling the excitation of the electrical machine. In the case

of Callia, the focus lies on smaller scale FPU, such as low scale hydraulic generators or Combined Heat-Power generators, with installed capacities up to a few MW [10].

- **Storage Systems (SS):** Storage systems are a key element in microgrids and a major flexibility provider for power grids. One common operation method for storage system is storing the surplus generation, when RES generation is too high and then to discharge it when the local demand is higher than the generation. Storage systems are seeing an increased use in MV and LV grids. There are several types of storage systems [14]. If a storage system is connected to the grid through a power inverter, the provision of reactive power could be possible. So far in Germany, some MW size storage systems are operating in the grids, connected to the HV grid.
- **Electric Vehicles (EV):** Electric vehicles are flexible by definition, as they act as mobile storage systems, which can be connected to different parts of the grid at different times. Traditionally, an electrical vehicle is the equivalent of a controllable load, but some use cases where EVs inject power back to the grid, to provide ancillary services, have been considered as well. Electric vehicles are seeing an increased use in Europe, but they are still not a reality in Turkey.
- **Reactive Power Compensation:** Reactive power compensation utilities, such as capacitor banks, STATCOMs or induction coils can inject or absorb reactive power, primarily to provide voltage support to power grids. This kind of compensation tends to be flexible, because they are built stepwise, where the grade of required compensation can be controlled. So far, there is no market value for reactive power, so the use of reactive compensation is seen so far as a cost-free solution for voltage control, thus its consideration remains outside the scope of Callia.

2.2 Linear Modelling of FPU

In both [6] and [8], the flexibility provision (defined as variables P_{flex} and Q_{flex}) of FPU is represented through rectangular limits for active and reactive power (see Type 1 boundaries in Figure 1). This provides a very simple representation for the flexibility limits, neglecting the direct dependency of active and reactive power limitations that happens in many cases (e.g. $\cos(\varphi)$ limits or technical limitations of inverters). To improve the representation of the operation range from typical grid utilities, five additional linear models are introduced. These models intend to provide an accurate representation of the PQ flexibility range of each kind of FPU. The objective is to provide the aggregation of the flexibility ranges measured at the DSO-TSO interconnection point. In order to improve the efficiency of the algorithm, a linear optimization problem is considered, forcing to obtain a linearized optimal power flow (OPF) model. The models show the technical limits of the corresponding FPU, based on specific technical parameters. In order to keep the linearity of the problem, all quadratic constraints are approximated by convex polygons, in order to ensure numerical convergence. It is possible to integrate other FPU models based on measurements or empirical values as well as new technologies, to the model, as long as they can be represented through convex polygons. The complete set of FPU models can be seen in Figure 1.

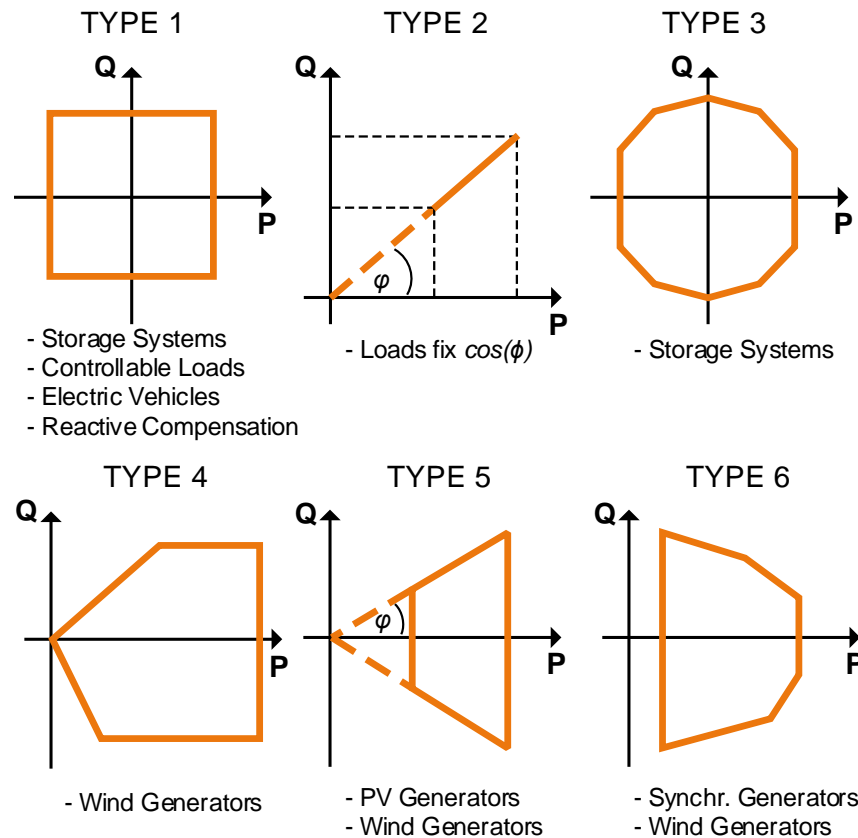


Figure 1: Operational restrictions of six types of FPUs [15].

3. Aggregation Model for Flexibilities

An algorithm to aggregate the flexibility range of a distribution grid was first elaborated within the EvolvDSO project [16] [8]. There, a nonlinear mixed-integer OPF optimization problem was formulated, in which the power flow through a predefined DSO-TSO interconnection point is optimized (e.g. a HV/MV transformer). The procedure aggregates the convex polygons delimiting the PQ boundaries of every FPU within the studied distribution grid. In order to improve the speed of the algorithm, some modifications are introduced in this work. The proposed optimization problem considers the linearization of the power flow equations and a set of linear convex constraints (limits of FPUs and limits of branches loading); therefore, the expected result is a convex polygon representing the overall flexibility of the grid. By linearizing the problem, the quickness of the algorithm can be strongly improved, with the trade-off that some accuracy may be lost. Figure 2 illustrates the aggregation process. Initially a power flow is performed, in order to obtain the prognosticated grid status. This is represented as the blue crosses within the FPU limits, showing the initial point of the calculation. The same can be seen for the aggregated value of the entire distribution grid (red cross). The aggregated flexibility range (area at slack node in Fig. 2) takes into account the grid state and corresponds to only such operation points, where no voltage band violations or overloaded power lines are present. Therefore, grid constraints (i.e. voltage and branch flow limits) are considered throughout the entire optimization process. More on the proposed methodology can be seen in [17].

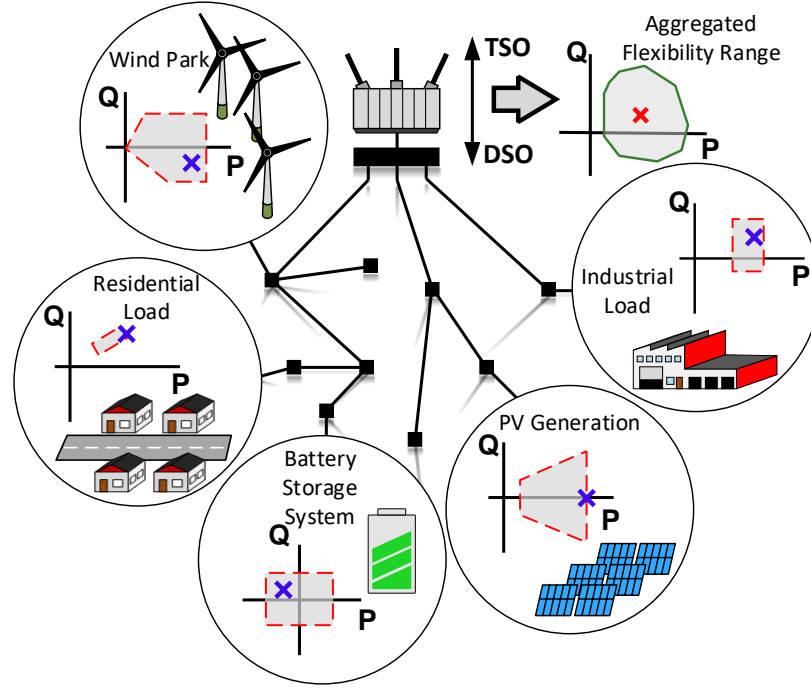


Figure 2: Schematic of flexibility aggregation process at the DSO-TSO interconnection point [17].

3.1 Linear flexibility aggregation methodology

The state of a power grid can be accurately represented through a set of nonlinear mathematical equations, which require large computational costs to solve, in case of larger grid models. The Newton-Raphson power flow method offers a way to reduce the required time to solve these equations. The objective of this paper is to provide a method that allows reducing the computational burden required to aggregate the flexibility of grids with a manifold of FPUs, based on the premises of the Newton-Raphson power flow. This chapter introduces a linear OPF model, constrained by the polygonal boundaries of FPUs, the node voltage limits and the linearized branch flow limits.

The objective function performs the aggregation of the FPU boundary polygons in one particular direction within a PQ Cartesian space. Therefore, only a meaningful set of possible solutions is explored. This includes the extreme scenarios with maximal generation and minimal load and vice versa. The proposed linear optimization method is formulated as a minimization problem using MATLAB's function '*linprog*', using the following formulation:

$$\min f^T \cdot x \text{ subject to } \begin{cases} A_{eq} \cdot x = b_{eq} & \text{Eq. (6)} \\ A \cdot x \leq b & \text{Eq. (13), (14)} \\ lb \leq x \leq ub & \text{Eq. (7)} \end{cases} \quad (3)$$

The state variables are the nodal voltages (magnitude and angle) and the active and reactive power set points of the FPUs (u , θ , P_{flex} , and Q_{flex}) and are contained in vector x . Parameters A_{eq} and A are matrices, while b_{eq} , b , lb and ub are vectors. The objective function f^T defines a line equation in a PQ Cartesian space that represents the active and reactive power exchanged through the slack node from or towards an over layered grid (i.e. through a MV/HV transformer). In the actual

condition, the model can only deal with grids that have single connections to the over layered voltage levels, thus have just one slack bus [8]. The complex branch flow $S_{slack,x} = P_{slack,x} + jQ_{slack,x}$ is defined as the power flow coming from the slack bus into the grid (based on Eq. (14)). By calculating the flexibility range of the grid, a set of coordinates $(P_{slack,x}, Q_{slack,x})$ are obtained, corresponding to the boundaries of the resulting range. The objective function of Eq. (3) is rewritten in terms of the branch flow over the slack node as:

$$f^T = \gamma \cdot (P_{slack,x} + \beta \cdot Q_{slack,x}) \quad (4)$$

The boundary points $(P_{slack,x}, Q_{slack,x})$ are obtained by maximizing or minimizing Eq. (4), which defines the direction of the operation in the PQ Cartesian plane. By setting γ to -1 or 1, the max. or min. optimization problem can be selected, and controlling β the direction in which the boundary points are searched can be defined. This allows the exploration in every direction from the grid operation point $(P_{slack,x0}, Q_{slack,x0})$. The process to obtain the linearized OPF model is explained in the following sections.

3.2 Linear Optimal Power Flow Equations

The nonlinear power flow equations in polar coordinates are the following [18]:

$$P_i(u, \theta) = u_i \cdot \sum_{j=1}^n Y_{ij} \cdot u_j \cdot \cos(\theta_i - \theta_j - \alpha_{ij}) \quad (5)$$

$$Q_i(u, \theta) = u_i \cdot \sum_{j=1}^n Y_{ij} \cdot u_j \cdot \sin(\theta_i - \theta_j - \alpha_{ij}) \quad (6)$$

It is possible to observe that voltages u_i and angles θ_i are tightly coupled. The traditional Newton-Raphson power flow (NR-PF) algorithm iteratively linearizes grid equations (5) and (6) using first order Taylor expansions. The algorithm iteratively optimizes the voltages on each node (u_i, θ_i) , by minimizing the difference $(\Delta P_i$ and $\Delta Q_i)$ between the calculated injected powers at each node with the actual injected power at the nodes, until they reach a defined tolerance limit. An iteration k of the NR-PF can be written, in terms of the Jacobian matrix J_k , as follows:

$$\begin{bmatrix} \Delta \theta_i \\ \Delta u_i \end{bmatrix}_{k+1} = \begin{bmatrix} \frac{\partial P_i}{\partial \theta} & \frac{\partial P_i}{\partial u} \\ \frac{\partial Q_i}{\partial \theta} & \frac{\partial Q_i}{\partial u} \end{bmatrix}_k^{-1} \cdot \begin{bmatrix} \Delta P_i \\ \Delta Q_i \end{bmatrix}_{k+1} = J_k^{-1} \cdot \begin{bmatrix} \Delta P_i \\ \Delta Q_i \end{bmatrix}_{k+1} \quad (7)$$

With each iteration, the Jacobian J_k in Eq. (7) is updated by correcting the values of u_i and θ_i , and then the inverse of the Jacobian (J_k^{-1}) is calculated. In order to be able to consider the flexibility provision of the FPU, the nodal balance equations need to be rewritten, to be able to account for the fixed and flexible power provision of every generator and load connected to node i (Eqs. (8) and (9)). The fixed part is the expected operation point of every utility, while the flex part is the flexibility provided by FPU (considering a pool of generators G , loads L and storage systems S). Active and reactive power flexibility provided by FPU are then added to Eqs. (8) and (9) as variables P_{flex} and Q_{flex} :

$$\Delta P_i = \sum_F (P_{fix,F,i} + P_{flex,F,i}) - P_i(u, \theta), F \in \{G \cup L \cup S\} \quad (8)$$

$$\Delta Q_i = \sum_F (Q_{fix,F,i} + Q_{flex,F,i}) - Q_i(u, \theta), F \in \{G \cup L \cup S\} \quad (9)$$

A grid with n nodes and m FPU requires $2n + 2m$ decision variables (u, θ for each bus and P_{flex}, Q_{flex} for each FPU). The voltage at the slack node can be freely selected, but requires being maintained constant during the aggregation process. In this case the voltage is set at 1 p.u. and angle 0° .

The NR-PF algorithm shows a very fast convergence in properly defined grids, requiring in most cases very few iterations to converge. One important requirement for the NR-PF algorithm to converge is that the Jacobian should be invertible and the problem should not be ill defined. Traditionally, a flat-start is a good initial guess ($u = 1$ p.u., $\theta = 0^\circ$ for every node). Providing an initial guess closer to the operation point of the grid would help the algorithm to converge even faster. This characteristic of the NR-PF is exploited here to linearize the power flow equations [19].

First, the state of the grid is determined through a standard NR-PF with P_{flex} and Q_{flex} set to zero for all FPUs. Prognoses of generation and load are used as inputs. The initial state vector x_0 is obtained this way with the resulting voltages. After the n^{th} iteration of the NR-PF algorithm, convergence is reached and the inverse of the Jacobian $J_{x_0} = J_n$ is defined as the linearization constant for the linear power flow model (Eq. (10)). The linearization occurs around the grid operation point obtained through the NR-PW calculation. The resulting linear grid model is expressed in terms of the state vector x as:

$$\begin{bmatrix} \Delta\theta_i \\ \Delta u_i \end{bmatrix}_x = \begin{bmatrix} \theta_i \\ u_i \end{bmatrix}_x - \begin{bmatrix} \theta_i \\ u_i \end{bmatrix}_{x_0} = J_{x_0}^{-1} \cdot \begin{bmatrix} \Delta P_i \\ \Delta Q_i \end{bmatrix}_x \quad (10)$$

According to the linear model obtained from Eqs. (9) and (10), any change to P_{flex} and Q_{flex} will cause the values of u_i and θ_i to change. This would cause the state vector x to drift around the initial state vector x_0 . Therefore, the error of linearizing the grid model around x_0 is expected to be smaller than when a flat-start is used as the linearization point. Finally, the magnitude of the nodal voltages u_i are constrained to:

$$u_{i,min} \leq u_i \leq u_{i,max} \quad (11)$$

One major disadvantage from the proposed method is that the Jacobian J_{x_0} is directly coupled with the admittance matrix Y that represents the grid model. This implies that any change in the grid topology, e.g. the operation of switches or an OLTC transformer, will cause changes to Y , thus having a direct impact on J_{x_0} and its inverse. Consequently, the tap position and switching operations cannot be considered as independent decision variables in the proposed model, as was the case in [8]. For each topology change, both matrices Y and J_{x_0} need to be recalculated, thus forcing to determine independent flexibility areas for each tap position. This statement applies to changes in the grid topology as well.

Branch flows are limited by the maximal apparent power of each branch, formulated through the following quadratic equation:

$$\sqrt{P_{ij}^2 + Q_{ij}^2} \leq S_{ij,max} \quad (12)$$

According to [18], Eq. (12) can be approximated through an n -sides regular polygons, without compromising the numerical stability of the optimization problem. The apparent power limit of each branch is then approximated piecewise by n segments defined as $L_{ij,k}$. The segments $L_{ij,k}$ define straight-line equations in the form of Eq. (13) (red dotted lines in Figure 3, with $k = 1, \dots, n$), where parameters a , b and c depend on angle α and the maximal branch flow $S_{ij,max}$.

$$L_{ij,k} = a_{ij,k} \cdot P_{ij} + b_{ij,k} \cdot Q_{ij} + c_{ij,k} \leq 0, \forall k = 1, \dots, n \quad (13)$$

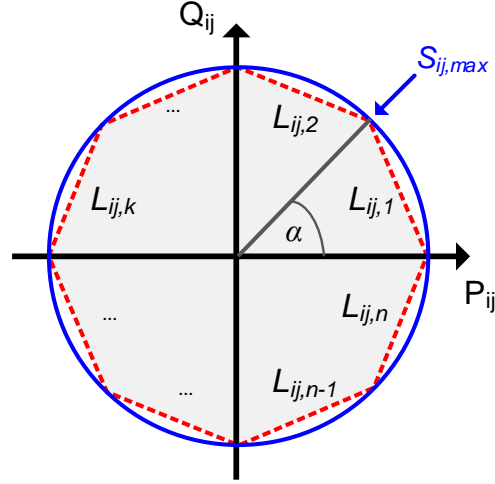


Figure 3: Piecewise linearization of the branch flow constraints [18]

The active and reactive power flow through the branch connecting nodes i and j , is defined as:

$$P_{ij}(u, \theta) = u_i \cdot Y_{ij} \cdot (u_i \cdot \cos(\alpha_{ij}) - u_j \cdot \cos(\theta_i - \theta_j - \alpha_{ij})) \quad (14)$$

$$Q_{ij}(u, \theta) = u_i \cdot Y_{ij} \cdot (u_i \cdot \sin(-\alpha_{ij}) - u_j \cdot \sin(\theta_i - \theta_j - \alpha_{ij})) \quad (15)$$

Eqs. (14) and (15) are nonlinear, requiring them to be linearized as was the case with Eqs. (5) and (6). The linearization process is similar as in the previous case, by calculating the Jacobian Matrix of Eqs. (14) and (15). The linearization operation point is the same as in Eq. (10). The linearized branch flow equations are defined in terms of the state vector x as follows:

$$\begin{bmatrix} P_{ij} \\ Q_{ij} \end{bmatrix}_x = \begin{bmatrix} P_{ij} \\ Q_{ij} \end{bmatrix}_{x_0} + \begin{bmatrix} \Delta P_{ij} \\ \Delta Q_{ij} \end{bmatrix}_x = \begin{bmatrix} P_{ij} \\ Q_{ij} \end{bmatrix}_{x_0} + \begin{bmatrix} \frac{\partial P_{ij}}{\partial \theta} & \frac{\partial P_{ij}}{\partial u} \\ \frac{\partial Q_{ij}}{\partial \theta} & \frac{\partial Q_{ij}}{\partial u} \end{bmatrix}_{x_0} \cdot \begin{bmatrix} \Delta \theta_i \\ \Delta u_i \end{bmatrix}_x \quad (16)$$

Linearizing around the operation point x_0 provides a much more accurate representation of the branch flows than a flat-start initialization, mostly due to a better representation of the grid losses. Coupling both Eqs. (13) and (16), a system of linear inequalities is obtained, which constrains the apparent power S_{ij} of each branch. These equation systems depend directly on the state vector x .

The boundaries of the FPU are like convex polygons, where each side of the polygon is modelled as a straight-line equation, according to Eq. (17). The state variables P_{flex} and Q_{flex} are constrained

by the polygons. Following this definition, a convex linear inequalities system is obtained for the FPU, in the following form:

$$a_{flex,i,t} \cdot P_{flex,i} + b_{flex,i,t} \cdot Q_{flex,i} + c_{flex,i,t} \leq 0 \quad (17)$$

Parameters $a_{flex,i,t}$, $b_{flex,i,t}$ and $c_{flex,i,t}$ define the segments t of the convex polygons defining each FPU connected to node i (based on the representation given in Figure 1).

3.3 Flexibility Aggregation Method

The methodology to determine the flexibility range of a distribution grid has basis on the ICPF algorithm proposed in [16]. The objective of the algorithm is to reveal the range of all feasible solutions for the exchanged power flow from and to the over layered grid through a defined slack node. This way the flexibility range of every FPU within the distribution grid is aggregated. The implementation of the algorithm allows only grid with just one interconnection point to be assessed, since the power flow over one interconnection point is optimized. Every solution provided by the aggregation method satisfies every grid voltage and line loading constraints, due to its OPF characteristic. The search algorithm assumes a convex solution space, since the constraints for the FPU are defined as convex polygons, so are the grid constraints [20].

The algorithm requires to know the specification of the technical limits of every FPU connected to the grid (based on Figure 1), including the connection point and if they are operating or not at that moment. The quality of the observability of the operation point of the FPU has a direct influence in the quality of the linearization of the grid model. Linearizing from the grid operation point, instead of a flat-start, improves the quality of the linearization.

During the first iteration of the assessment of the flexibility range, the extreme boundary points P_{max} , P_{min} , Q_{max} and Q_{min} are obtained by minimizing and maximizing the objective function in Eq. (4). For this purpose, the parameter β is defined as 0 or ∞ . In Figure 4, a schematic representation of the aggregation algorithm is shown. The intersection of the straight lines connecting the boundary points $P_{min} - P_{max}$ and $Q_{min} - Q_{max}$ defines four search quadrants (defined as I-IV). The parameter β is automatically calculated as the slope of the straight lines connecting adjacent boundary points (red dotted lines in Figure 4). Within a quadrant, the slopes β have the same sign. In Table 1, the signs of β and γ in Eq. (4) are defined for each search quadrant. A flowchart of the proposed algorithm can be seen in Figure 5.

Table 1: Objective function components by quadrant

Quadrant	I	II	III	IV
sign(β)	-	+	-	+
γ (Eq. (17))	1	-1	-1	1

Figure 5: Flow chart of the linear flexibility range aggregation algorithm [17].

Having computed the first set of β (red dotted lines in Figure 4), the iterative exploration of the quadrants is initiated. The second iteration results in the green triangles and the third iteration results in the blue squares in Figure 4. All four quadrants can be explored independently and in parallel. For each iteration, the obtained boundary points in all quadrants are reorganized by reactive power value (from higher to lower). Points located too close to each other, within a predefined range ε , are discarded in order to avoid the algorithm to search repeatedly on the same spot. Subsequent iterations repeat the search process using new values of β , calculated from the new sets of boundary points. The process stops after a predefined amount k_{max} of iterations.

In [8], the search algorithm converges when the difference in the angle ϕ between all adjacent segments is below a predefined threshold. This can also be seen as the difference between the slopes β of two adjacent segments is small enough. This would allow obtaining a smooth contour, but the algorithm may not converge, if the solution space contains sharp-edges. In this version of the algorithm, the maximum amount of iterations is predefined, in order to maintain a constant processing time and to disallow unnecessary iterations that could occur, if the maximal angle difference is not reached (which may happen when sharp edges exist). After k_{max} iterations, $2^{k_{max}+2}$ contour points are obtained ($2^{k_{max}-1}$ for each quadrant). It was observed that $k = 3$ iterations tend to be sufficient to obtain a representative approximation of the aggregated flexibility range (meaning that a maximal amount of 32 boundary points are obtained). The resulting contour is the convex hull defined by the boundary points after the last iteration (e.g. blue lines in Figure 4).

At this stage, the algorithm expects a full knowledge of the grid topology, since both Eq. (10) and Eq. (16) are tightly coupled to the admittance matrix Y , which represents the grid topology. If this grid topology changes, i.e. due to the switching on and off power lines and transformers, or due to the change in the tap position of an OLTC transformer, the admittance matrix will change as well, modifying the structure of the OPF formulation. Each change in the grid topology would force to perform an entirely new calculation of the flexibility range. Optimized ways to deal with these changes in the grid topology are an active research topic (see [21]).

3.4 Flexibility Aggregation over Different Voltage Levels

The aggregation of the flexibility range at a DSO/TSO interconnection point using nonlinear mathematical methods becomes a very complex computational problem when large quantities of FPU are involved. This represents a challenge for grid planners, since the consideration of large amounts of FPU is required during the planning process. The linear OPF model proposed in [17] reduces the computational burden involved in the aggregation of the grid flexibility, considering grid constraints. The usage of this linear model allows considering its usage as an information exchange method between grid operators. Since grid operators usually control different voltage levels of the grid, such an information, like the flexibility range of a grid could be useful to facilitate this trade.

Here, the linear model is used to aggregate different voltage levels within a distribution grid (which could represent the interconnection point between grid operators), following many stages of aggregation. In this case, an MV grid with several LV grids is considered. The mathematical description of the linear aggregation method was already explained in Chapter 5.3. First, the

flexibility provided by each LV grid is aggregated at an individual basis. The obtained flexibility ranges for each LV grid are added to the MV grid as non-regular FPU. This allows the aggregation of the flexibility provided by the entire MV grid to an HV grid, allowing the reduction of the dimensionality of the optimization problem for the MV grid, since the LV grids are now provided in an aggregated way. Special attention needs to be given to the voltages at the connecting nodes of the LV grids, since the voltage profiles of the MV grid have a strong influence on the LV grid. Figure 6 exemplifies the proposed multi-level aggregation method with a 20kV MV distribution grid with three different 0,4kV LV grids connected to it, which are aggregated and represented as a flexible load [22]. The multi-stage aggregation methods are detailed in this chapter. A more detailed explanation of the procedure and the results of the research can be found in [15].

Step 1: Aggregation of Single LV Grids

In a first stage, each LV grid is considered as an individual grid, where the connection to the MV grid is modelled as an infinite bus (slack node). The power flow through the 20/0.4kV transformers is aggregated taking into account the flexibility provision of all FPU connected at the LV level. By applying the linear aggregation method of [17], independent flexibility ranges for each one of the LV grids are obtained. Each LV grid offers a different amount of flexibility to the grid, depending of the kinds of FPU connected to it, as well as the own LV grid topology.

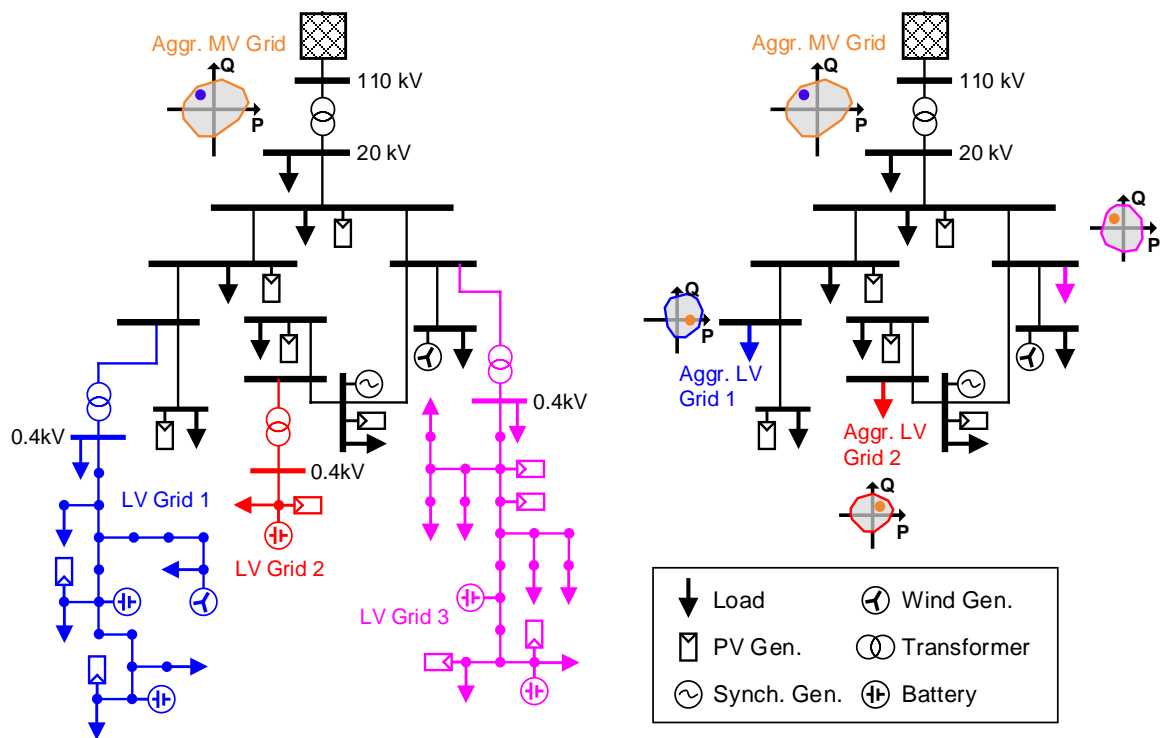


Figure 6: Flexibility aggregation scheme of a MV distribution grid containing different LV grids [22].

Step 2: Aggregation of MV Distribution Grid

The aggregation of the LV grids results in non-regular convex polygons representing their flexibility. These polygons are defined as FPU within the MV grid, characterized as loads, limiting the operation points of the LV grids. Adding the LV grid FPU to the MV grid model allows performing the next stage of the aggregation, using the same methodology as in the first step. Using this

methodology, the provision of flexibility by each LV grid can be assessed independently, as well as its impact in the overall flexibility provision of the MV grid.

One issue arises during the proposed aggregation methodology, involving the voltages at the interconnection points. The aggregation method in [17] states that the voltage at the slack bus needs to be kept constant (typically $u = 1$ p.u., $\theta = 0^\circ$). This statement is no longer valid if more voltage levels are considered, since the voltage at the interconnection points will fluctuate during the aggregation process of the MV grid, thus influencing the voltage profiles of the under-layered grids. This may cause a poor estimation of the flexibility range of the MV grid, mostly regarding the reactive power values. The search for solutions of this problem is an active research topic. An iterative process would be required to solve this issue, where the voltages at the MV level are transferred to the LV levels and given as a starting point for their aggregation. This solution goes against the initial bottom-up proposal of the algorithm, but could help mitigate errors in the calculation.

4. Case Study for Callia

4.1 Grid Model Definition

The proposed flexibility aggregation method is verified using an adaptation of an urban distribution grid feeder within the control zone of the DSO Stadtwerke Heidelberg Netze in Germany. The distribution grid in the City of Heidelberg comprises a 110kV network with 20kV MV feeders. The distribution grid is connected through 220/110 kV transformers to the transmission grid control zone of the TSO TransnetBW. Each 20kV MV feeder is fed through a 110/20 kV OLTC transformer. For the purpose of the present deliverable, a reduced grid model with 67 nodes was developed, representing an abstraction of the grid data provided by the Stadtwerke Heidelberg Netze. In Figure 7, a schematic representation of the designed grid model is shown. The figure details the nodes with distributed generation connected to them.

A list detailing the generation and load characteristics of the grid can be found in Table 2. A set of FPU were defined for this grids, according to the flexible generation units existing in the grid. In a first stage, to test the effectiveness of the algorithms, every load in both grids is considered to be an FPU, able to reduce its consumption up to 10%. The distribution of the FPUs within the grid can be seen in Figure 7.

Table 2: Characterization of the 67 nodes MV distribution grid

Parameter	MV Grid 1		MV Grid 2		HV Grid	
	MW	MVAr	MW	MVAr	MW	MVAr
Total Installed Load	11,95	3,93	23,59	7,75	151,54	11,68
Total Installed Generation	4,7	0	8,21	0	12,9	0
Grid Losses	0,015	0,19	0,123	0,62	0,462	7,51
Cables Capacitance	0	-0,5	0	-0,5	0	-51,5
Power Flow at the Slack Generator	7,28	3,69	15,52	8,09	139,2	3,1

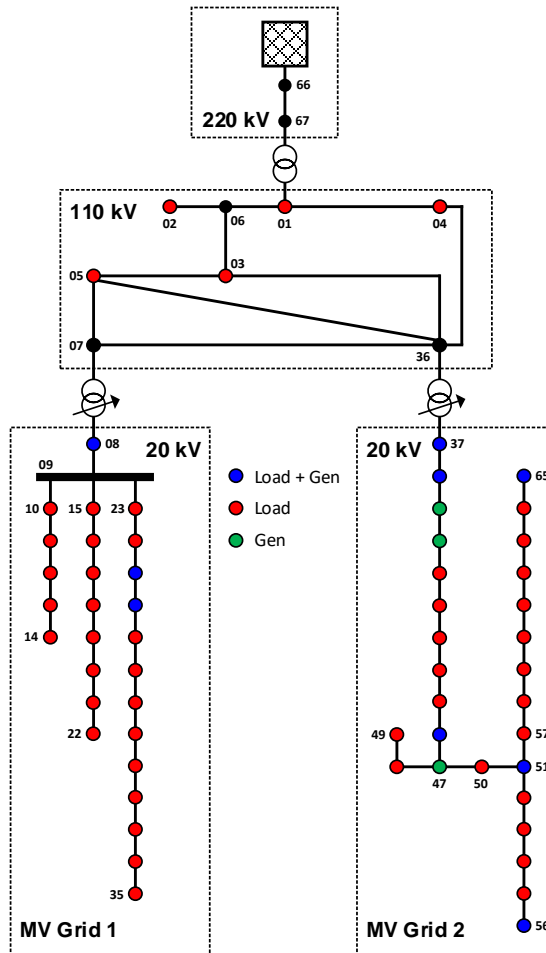


Figure 7: Schematic representation of the 67 nodes distribution grid.

Table 3: Distribution of FPU's in the studied 67 Nodes MV distribution grid

Grid	FPU Type						Total
	1	2	3	4	5	6	
MV Grid 1	0	27	0	0	2	0	29
MV Grid 2	0	25	0	0	5	3	33
HV Grid	0	52	0	0	7	3	62

4.2 Flexibility Aggregation

In this section, the proposed methodology to aggregate the grid flexibility is applied to the previously defined distribution grid of Figure 7. Every generator is considered able to provide flexibility to the power grid, including reactive power capability. Within the distribution grid, the loads are considered to be able to reduce instantaneously their consumption in maximal 10%, while maintaining a fix $\cos(\varphi) = 0,95_{ind}$. The proposed aggregation algorithm is implemented in two different ways, first by aggregating the entire grid at once, considering all voltage levels simultaneously, and second by performing a two-step aggregation, where the MV voltage grids are first aggregated independently and their flexibility range is given as an input for the HV grid. A comparison of the results obtained for both cases is given.

The voltage limits of the grid are set to $\pm 10\%$ from the nominal value for every node. The performed simulations consider cases where the OLTC is both active and inactive. The branch flows limits were approximated using $n = 8$ linear equations in the form of Eq. (11). The proposed algorithm was tested using a ‘Dual Simplex’ solver without any parallelization of the search procedure. Simulations were performed using MATLAB on a laptop with an i5-6300U 2.4GHz processor, 8GB RAM and a 64 Bits Windows 10 operating system.

a. One-Step Aggregation:

The results of the one-step aggregation can be seen in Figure 8, where the grid can provide around 4,2 MW of active power flexibility and 5MVar of reactive power flexibility. It is possible to distinguish the non-rectangular shape of the flexibility range, given the way the FPU are modelled. Every operation point between the delimitations is considered a valid operation point of the grid. In Figure 9, it is possible to see that the combination of set points that generate the flexibility area of Figure 8 do not violate any voltage constraints within the grid. The orange lines mark the maximum and minimum voltages at each node of the grid. Under the considered operation point of the grid, no combination of active and reactive power provided by the FPUs could cause the voltage to drop below 0.9 p.u., similar to what happens to the loading of cables. The voltage limits are set to $\pm 10\%$ from the nominal value, according to [23].

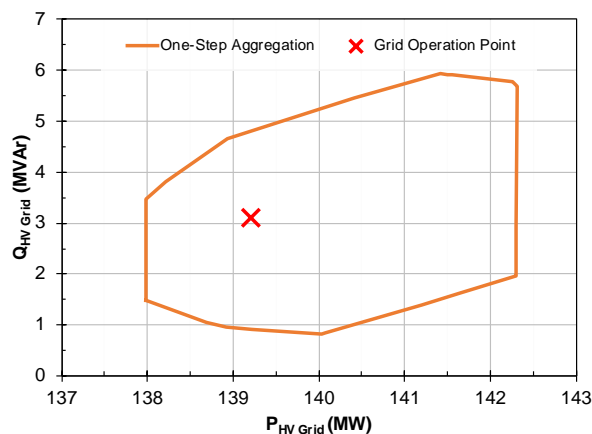


Figure 8: Flexibility range at the TSO/DSO interconnection point using one-step aggregation.

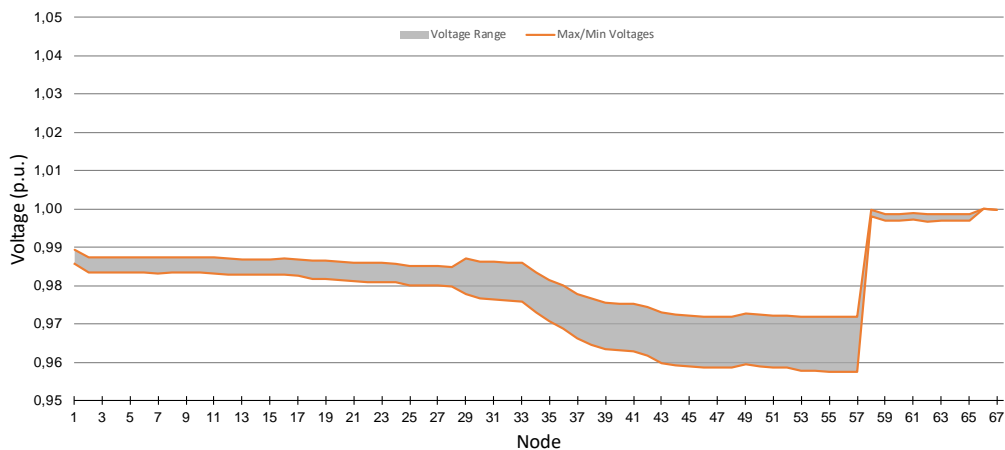


Figure 9: Voltage band of each grid node resulting from the aggregation process.

b. Two-Step Aggregation:

The two-step aggregation begins with the separation of the entire grid into three regions, the HV region and the two MV regions. First, the MV grids are aggregated independently, resulting in the flexibility regions of Figure 10 and Figure 11. It can be perceived that the MV Grid 1 offers very little flexibility, mostly due to the existence of only two small PV generators in the region, as well as a smaller amount of load than MV Grid 2. The MV Grid 2 contains two large CHP generators, which mostly dictate the flexibility of the grid. These resulting areas are given to the HV grid model as FPU. The result of the second step of the aggregation can be seen in Figure 12. There is a slight difference in the results obtained with both methodologies, which relates to a difference in the operation point given for the grid in both cases. This issue is related to the voltage fluctuations at the interconnection points. During the first part of the aggregation process, the voltage at the interconnection bus was set at 1 p.u. In Figure 9, it can be seen that there is a voltage band at nodes 1 and 29 (the 110/20kV interconnecting nodes), which would change the voltage at the slack bus for the second step of the aggregation process. This issue was already discussed in [15]; only in this case, there are no violations of the voltage limits within the 20 kV grid, as could be seen in Figure 9.

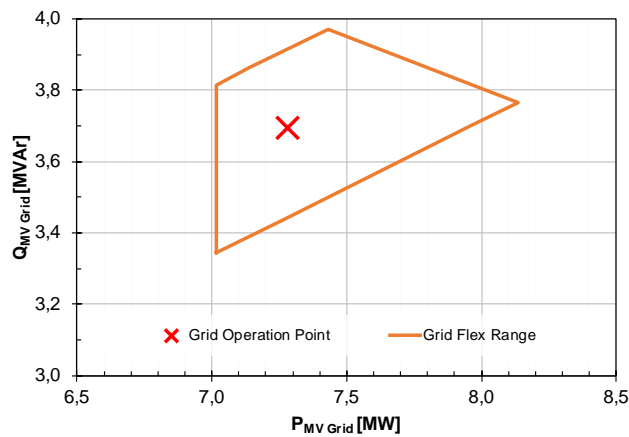


Figure 10: Flexibility range at the HV/MV interconnection point of MV Grid 1.

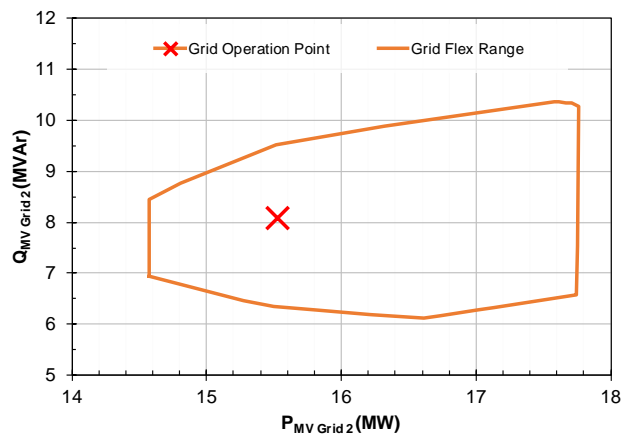


Figure 11: Flexibility range at the HV/MV interconnection point of MV Grid 2.

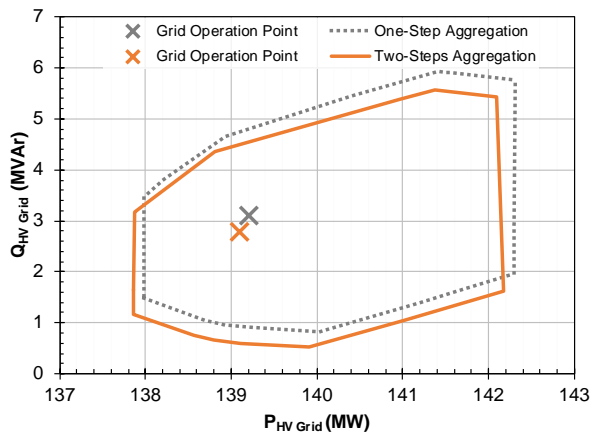


Figure 12: Comparison of flexibility ranges at the TSO/DSO interconnection point using one- and two-step aggregations.

4.3 Callia Use Cases

a. Congestion Management

In CALLIA, a congestion in the grid is described as an overload of a power line or a cable, where the transported power is equal to or higher than the maximal allowed power, before the equipment can suffer any structural damage due to large currents. The load of power line is calculated according to Eq. (1). For the studied grid model, no cases of congestion are detected, since the loading of the grid is lower than its capacity. The critical path where congestions may arise, if the load increases, is the branch connecting nodes 37 to 47, within the MV Grid 2. While performing the aggregation of the flexibilities in the grid, its influence on the line connecting nodes 38 and 39 is observed (orange polygon in Figure 13). This is one of most loaded lines in the grid, where even after changing the operating point of all components in the grid, the operational limit is not reached in any way (gray line in Figure 13).

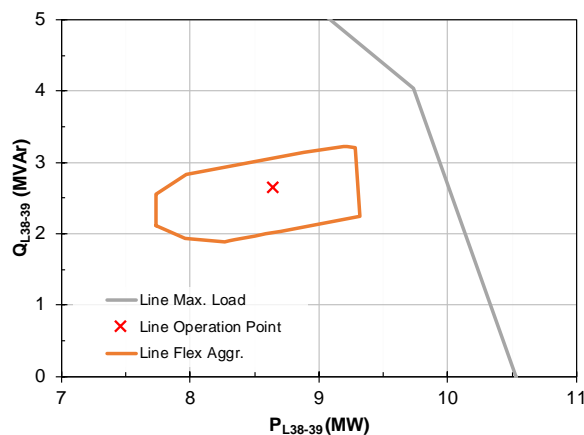


Figure 13: Loading of line 38-39 while performing the flexibility aggregation.

To be able to see the effect of a congestion in the grid, the maximum rate of the power lines in the grid was linearly reduced with a scaling factor of 0.88. The results of this change in the grid can be observed in Figure 14, where the operation point of the power line is now located outside the valid

area. In order to show the usage of storage systems as a measure to reduce congestions, a fictitious scenario was designed, where three identical battery storage systems of 200kW are connected to the grid. In this scenario, no flexible loads and generators are considered, just the batteries, which are connected to the grid at nodes 49, 52 and 59. The aggregation of the flexibility provided by these batteries can be seen in Figure 14, with and without the consideration of the grid constraints. The batteries could provide enough flexibility in order to bring the operation point back into the valid area, which would require the batteries to operate as generators, thus injecting power into the grid. This can be seen in Figure 15, where the operation charts of the three batteries are shown. It can be observed in Figure 15, that the specified operation point for the batteries would cause an invalid operation point of the entire grid, due to a violation of the branch limit of L38-39, as shown in Figure 14.

If the grid constraints would not be considered, all batteries could work in all four quadrants, but the grid constraints only allow them to work as generators, while in the case of batteries 1 and 2, even the reactive power provision is limited, in order not to affect the grid constraints. The required power to bring the line back to a valid state can be obtained many combinations of these batteries, where around 100kW of power are required to be provided by the batteries to return to the valid state. When the set point of one of the batteries is redefined (e.g. Battery 1 provides 100kW to the grid), the flexibility range of the other two batteries need to be recalculated, since the operation point of the grid is changed.

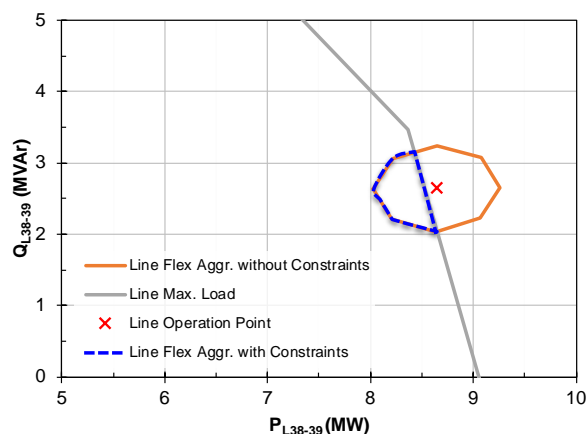


Figure 14: Loading of line 38-39 while performing the flexibility aggregation with reduced grid capacity

In reality, market mechanisms do not take the grid constraints into consideration during their clearing, therefore they would be able to sell both the positive and negative power of these batteries (depending on their state of charge). In this case, it can be seen that a provision of negative power would strongly threaten the security of the power line. It is to be noticed, that in this case, with only top-down power flows, only the usage of generating FUs connected at the end of the branches could help with the congestion management. The concept of intra-DSO trading applies very well to this case.

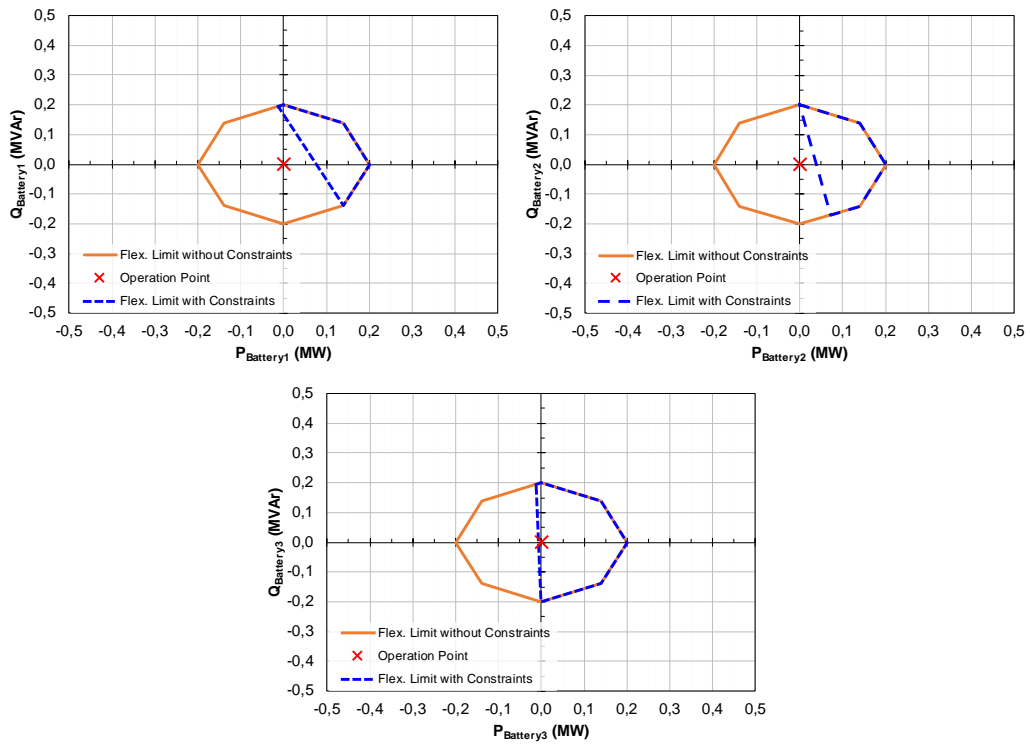


Figure 15: Operation charts of three batteries while performing the flexibility aggregation with reduced grid capacity

b. Local Balancing

There is no specific definition for a balancing zone, therefore, in this case the local balancing is considered as the invariance of the power flow through the 110/220kV transformer in Figure 7. Any usage of flexibility within the grid should be compensated by another flexibility within the grid, thus ensuring that the flow through the transformer stays constant. Balancing can be perceived as an equalization of either power or energy, depending on the relevance of time as a decision variable. In this case, it is investigated, if the usage of flexibility within one MV grid can be compensated with regard to the system balance in the second MV grid, by just considering a single time step.

In Figure 16, the flexibility provision of both MV grids for the investigated case study is shown. The operation point was subtracted in order to show the values of ΔP and ΔQ that both grids can supply to the HV grid. The max branch flow constraints were reduced with a factor of 0.88, in order to show their effect on the aggregation of the grid (especially in MV grid 2). It can be appreciated that the MV grid 2 can provide enough flexibility to cover any requirement of MV grid 1, but the opposite cannot be ensured. Only flexibility requirements located within the intersection of the flexibility area of MV Grid 1 with the mirrored flexibility area of MV Grid 2 could be covered without violating the local balancing. Any requirement outside the limits of MV grid 1 would force the grid to import or export energy from the TSO grid.

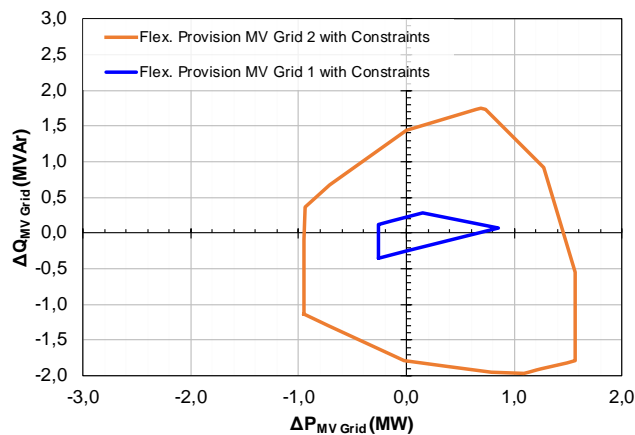


Figure 16: Flexibility provision of both MV grids, considering the operation of three batteries and reduced grid capacity

c. Grid Losses Mitigation

Some of the energy transported through power lines will be lost in the process, mostly in the form of heat. The more a power line is loaded (more current flowing through the line), the larger will these grid losses be (see Eq. (2)). Grid losses could be reduced by reconfiguring the active power flows in a grid, which should result in a homogenization of the flow through the entire grid. One simple way to achieve this, is by reconfiguring the grid topology. By closing open rings, the voltage profiles on both branches are levelled, therefore the power flows are homogenized and grid losses can be reduced [24]. This solution has no market value so far, since a grid operator can perform it directly just by connecting or disconnecting a switch, without involving other actors. According to [24], in general cases, closing an open ring in an MV grid can help reduce grid losses in 4%-10%, depending on the load scenario and the grid topology.

Here, the effect over the grid losses caused by modifying production and consumption of FPUs is assessed. During the flexibility aggregation process presented in the previous chapter, the sum of the active power losses of each power line was calculated for each iteration. This way, the total grid losses for different FPU set point combinations is obtained. The distribution of the results for a single load scenario is shown in Figure 17.

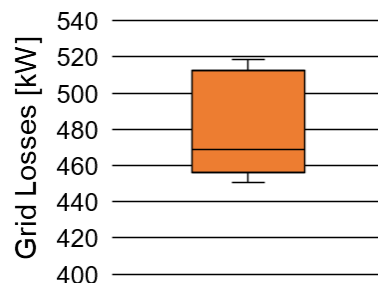


Figure 17: Distribution of cumulated grid losses for the operation points obtained from the flexibility aggregation process.

By varying the generation and consumption of the FPUs, the power flow at the DSO/TSO interconnection point is changed. For the studied scenario, the grid losses are situated at 462 kW at the operation point. During the aggregation process, they can be located between 450 kW and

520 kW. The variation of the grid losses against the variation of the power flow at the interconnection point was computed (both values regarding the grid operation point, obtained from Table 2) based on Monte-Carlo simulations with random set points of each FPU, using 10.000 iterations. For the sake of simplicity, each FPU was considered as type 1 (according to Figure 1), using the same set of restrictions for the maximal and minimal values than during the aggregation process. In a first scenario, the set-points of the loads was modified between 0% and 120% of the provided set point, while the restrictions to the generation units suffered no modification (Figure 18). In a second scenario, the set points of the generation units could be set between 0% and 200%, while all loads were considered as static (Figure 19). Both plots show the difference between the described variations of the set points of the grid components with the results for the initial set point described in Table 2.

It can be noticed, that by keeping the active power flow at the interconnection point constant, a grid losses reduction of around 23 kW could be reached. This would represent one variant of the local balancing use case.

In Figure 18 it can be seen that disconnecting every load in the grid would decrease the grid losses by 180kW, but at the cost of shedding 13 MW of load. Something similar occurs in Figure 19, where the grid installed generation is duplicated, reducing grid losses by 56 kW, by increasing generation by 3MW. This shows that in MV grids, the potential of reduction of grid losses is not really significant and would require shedding large amounts of loads or increasing generation significantly, which in both cases could involve more costs, than just covering the grid losses.

Under these circumstances, the use case of losses mitigation should be considered as a constraint to the overall flexibilities problem, where a solution of the Callia market platform should ensure the lowest grid losses as possible. The incurrence of larger grid losses by dispatching the FPUs in non-optimal ways could be minimized by means of penalty functions among the optimization problem. The use of flexibilities to reduce grid losses does not offer many advantages than e.g. modifying the grid topology.

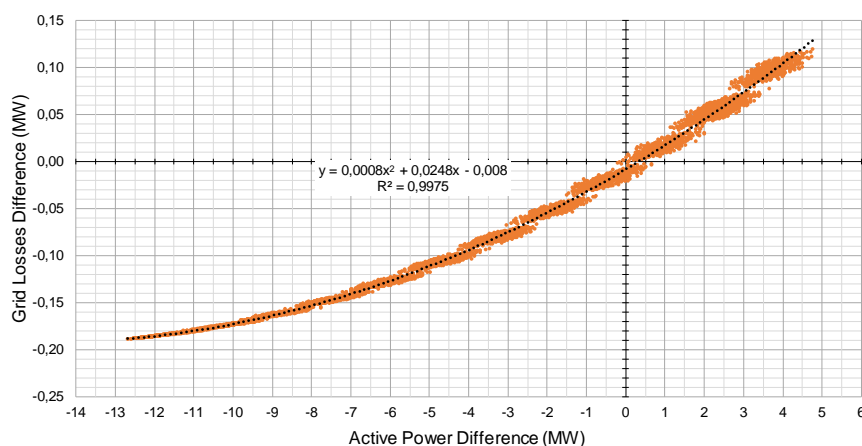


Figure 18: Variation of grid losses in terms of the variation of the active power flow through the DSO/TSO interconnection point with installed load between 0% and 120%.

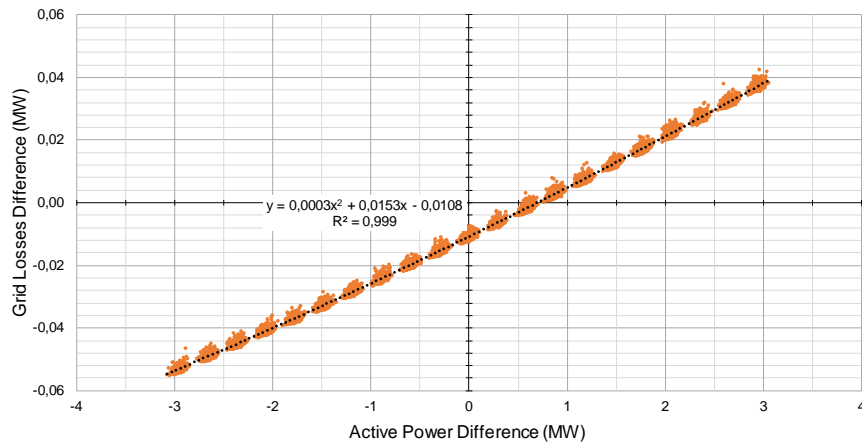


Figure 19: Variation of grid losses in terms of the variation of the active power flow through the DSO/TSO interconnection with generation installed power between 0% and 200%.

d. Voltage Control

The use case for voltage control focuses on the provision of reactive power flexibility to the power grid. In reality, the most used methods to control the voltage profiles of the grid are static reactive power compensators (coils and capacitors banks) and the usage of OLTC transformers. In this chapter, the usage of reactive power flexibility will be compared to the usage of an OLTC transformer.

If the tap position of an OLTC transformer is changed, the reactive power flexibility provision of the grid changes accordingly, as was demonstrated in [21].

The voltage bands of each node during the aggregation process, with the OLTCs as flexibility providers, can be seen in Figure 20 and Figure 21. In the graphics, the influence of the tap changer can be seen by the blue dashed lines, while the gray area shows the influence of the tap changer and the flexibility provision of the FPU. As expected, the tap changers have a very strong influence on the voltage profiles, much larger than what the reactive power flexibility provision can provide. A joint usage of the tap changer and the provision of reactive power flexibility could be foreseen to maintain the grid voltage between certain established limits, which could be more restrictive than [23]. Tap changers work with discrete steps, therefore the flexibility range of the voltage in Figure 20 and Figure 21 would not be entirely reachable, as there should be some breaks between each tap position, as was already demonstrated in [21].

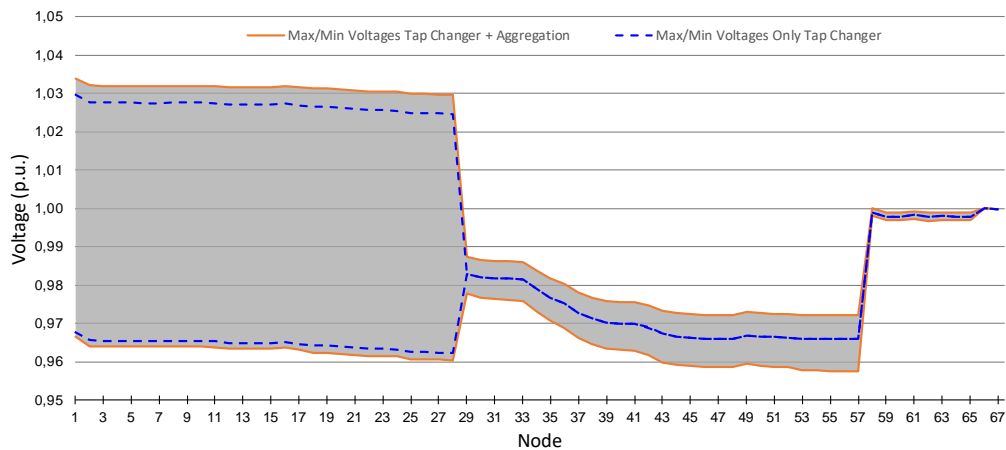


Figure 20: Voltage bands of each grid node during the aggregation process considering OLTC transformer in MV Grid 1 (between +4% and -2% voltage change).

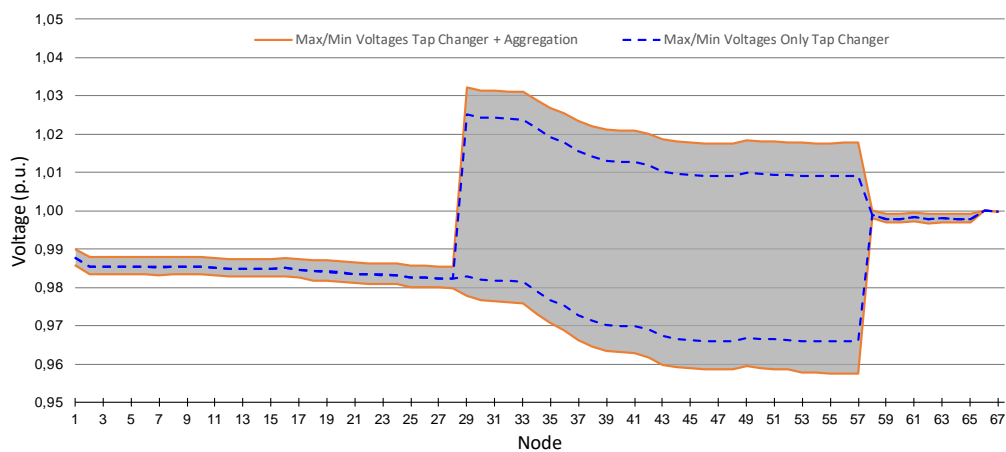


Figure 21: Voltage bands of each grid node during the aggregation process considering OLTC transformer in MV Grid 2 (between +4% and -2% voltage change).

As was the case with the loss mitigation use case, this use case is not seen as promissory for the use of flexibilities. Although reactive power is relevant for the control of voltage in the grid, large amounts of it are required to cause significant changes in the voltage profiles. Nowadays reactive power compensation is provided by large synchronous generators and reactive power compensators (several MVar). Distributed generation only provides a small share of the reactive power quantities required to keep the voltage levels stabilized. Another aspect to be considered is that nowadays there is no formal market for reactive power. The control of the voltage profiles in the grid could be considered as a constraint for the clearance of a flexibility market algorithm, which tries to ensure that every node is operating within allowed limits.

5. Conclusions

This deliverable elaborates on the use of flexibilities to deal with the problems of penetration of DER. A linear optimization model for the aggregation of active and reactive power flexibility of distribution grids at a TSO-DSO interconnection point was presented. The power flow equations were linearized by using the Jacobian matrix of the Newton-Raphson algorithm in a smart way. The model was complemented with non-rectangular linear representations of typical FPU, increasing

the accuracy of the distribution grid aggregation. The obtained linear programming system allows a considerable reduction of the required computing time for the process. At the same time, it maintains the accuracy of the power flow calculations and increases the stability of the search algorithm while considering large grid models.

The algorithm was tested in an abstraction of an urban distribution grid in Heidelberg, Germany, in scenarios with high quantity of FPU's. The model was implemented using linear programming tools in MATLAB. In a scenario with more than hundred FPU's, the proposed model shows its fortitudes, requiring just less than 3% of the computing time than the original nonlinear model in the case of the largest tested grid (considering the ICPF algorithm of [16]). The quality of the solution shows very little variation from the nonlinear model. This variation of the algorithm is promising and has the potential to be further developed and improved, offering an effective tool to advance in the study of the utilization of flexibilities in distribution grids.

The developed method can have many practical applications, which could improve the coordination between grid operators. It can help evaluate the effect of the activation of flexibilities by TSO's located within DSO grids (e.g. for frequency control purposes). The impact of flexibility markets could be observed by including market results as constraints in the OPF model. Distribution grids operating at more than one voltage level can be represented by the aggregation of the results acquired from the single feeders, therefore reducing the need to declare sensitive grid information.

Within CALLIA, four different use cases for the use of flexibilities were identified. In the case of congestion management, it was shown that flexibilities could play a very important role in relieving them by modifying the power flows within the grid. This can be considered together with the concept of local balancing, where any activation of flexibility needs to be compensated in order to maintain the equilibrium between load and consumption in the grid. It was shown, that two different grids could cooperate to provide local balancing, only if they can provide similar amounts of flexibility. At a larger scale, this compensation could be distributed throughout several grids.

In the case of loss mitigation, the usage of flexibilities does not show better results in comparison to using cost-free methods, i.e. topology reconfiguration. Large amounts of flexibilities are required to reach noticeable reductions in grid losses. This could be considered as a constraint to the local balancing problem, where the optimal solution should ensure minimal grid losses. An extreme scenario would involve a very strong local balancing, where autarchy is the norm, but the power grid is not getting into that direction for the time being. Finally, in the case of voltage control, taking a large synchronous generator out of service, i.e. a nuclear plant or a coal plant, requires too many small DER units as replacement, whose provision of reactive power is reduced. It was shown, that the use of a OLTC transformer plays a much larger role in keeping voltage profiles stabilized, than providing reactive power flexibility from FPU's.

For the development of Callia, an initial approach considering the use cases of congestion management and local balancing should be pursued. The other use cases can be incorporated at later stages as supplementary approaches, which could help improve the quality of supply by grid operators.

Bibliography

- [1] S. Ruester, S. Schwenmen, C. Batlle en I. Pérez-Arriaga, „From Distribution Networks to Smart Distribution Systems: Rethinking the Regulation of European Electricity DSOs,” *Utilities Policy*, vol. 31, pp. 229-237, 2014.
- [2] EURELECTRIC, „Active Distribution System Management,” February 2013. [Online]. Available: http://www.eurelectric.org/media/74356/asm_full_report_discussion_.
- [3] R. Bärenfänger, E. Drayer, D. Daniluk, B. Otto, E. Vanet, R. Caire, T. Shamsi Abbas en B. Lisanti, „Classifying Flexibility Types in Smart Electric Distribution Grids,” in *CIREC Workshop*, Helsinki, Finland, 2016.
- [4] EDSO, „Flexibility: The role of DSOs in tomorrow’s electricity market,” 2014. [Online]. Available: <https://www.edsoforsmartgrids.eu/wp-content/uploads/public/EDSO-views-on-Flexibility-FINAL-May-5th-2014.pdf>.
- [5] H. Gerard, E. Rivero en D. Six, „SmartNet D1.3: Basic models for TSO-DSO coordination and ancillary services provision,” [Online]. Available: http://smartnet-project.eu/wp-content/uploads/2016/12/D1.3_20161202_V1.0.pdf.
- [6] N. Fonseca en et al., „EvolvdSO Grid Management Tools to Support TSO-DSO Cooperation,” in *CIREC*, Helsinki, Finland, 2016.
- [7] M. Heleno, R. Soares, J. Sumaili, J. BessaR., L. Seca en M. A. Matos, „Estimation of the Flexibility Range in the Transmission-Distribution Boundary,” in *PowerTech*, Eindhoven, Netherlands, 2015.
- [8] J. Silva en et al., „Estimating the Active and Reactive Power Flexibility Area at the TSO-DSO Interface,” *IEEE Transactions on Power Systems*, 2018.
- [9] H. Chen en A. Moser, „Improved Flexibility of Active Distribution Grid by Remote Control of Renewable Energy Sources,” in *International Conference on Clean Electrical Power*, Liguria, Italy, 2017.
- [10] M. Braun, „Provision of Ancillary Services by Distributed Generators,” University of Kassel, Kassel, Germany, 2008.
- [11] A. Ellis en et al., „Reactive Power Performance Requirements for Wind,” in *IEEE PES General Meeting*, San Diego, USA, 2012.
- [12] I. Erlich, M. Wilch en C. Feltes, „Reactive Power Generation by DFIG Based Wind Farms with AC Grid Connection,” in *IEEE Powertech*, Lausanne, Switzerland, 2008.
- [13] G. K. Irungu, A. O. Akumu en D. K. Murage, „Modeling Industrial Load Due to Severe Voltage Surges and Sags: ‘A Case Study of Magadi Soda Company’,” in *AFRICON*, Windhoek, South Africa, 2007.
- [14] L. Chang, W. Zhang, S. Xu en K. Spence, „Review on Distributed Energy Storage Systems for Utility Applications,” *CPSS Transactions on Power Electronics and Applications*, vol. 2, nr. 4, pp. 267-276, 2017.
- [15] D. Contreras, O. Laribi, M. Banka en K. Rudion, „Assessing the Flexibility Provision of Microgrids in MV Distribution Grids,” in *CIREC Workshop*, Ljubljana, 2018.
- [16] E. Rivero, D. Six, A. Ramos en M. Maenhoudt, „Deliverable 1.3 - Preliminary assessment of the future roles of DSOs, future market architectures and regulatory frameworks for network integration of DRES,” 2014. [Online]. Available: <http://www.evoldso.eu>.
- [17] D. Contreras en K. Rudion, „Improved Assessment of the Flexibility Range of Distribution Grids Using

Linear Optimization,” in *PSCC 18*, Dublin, Ireland, 2018.

- [18] Z. Yang, H. Zhong, Q. Xia, A. Bose en C. Kang, „Optimal Power Flow Based on Successive Linear Approximation of Power Flow Equations,” *IET Generation Transmission Distribution*, vol. 10, nr. 14, pp. 3654-3662, 2016.
- [19] S. Bolognani en S. Zampieri, „On the Existence and Linear Approximation of the Power Flow Solution in Power Distribution Networks,” *IEEE Transactions on Power Systems*, vol. 31, nr. 1, pp. 163-172, 2016.
- [20] O. Krause, S. Lehnhoff, E. Handschin, C. Retanz en H. F. Wedde, „On feasibility boundaries of electrical power grids in steady state,” *Electrical Power and Energy Systems*, vol. 31, pp. 437-444, 2009.
- [21] J. Silva, J. Sumaili, R. J. Bessa, L. Seca, M. Matos en V. Miranda, „The challenges of estimating the impact of distributed energy resources flexibility on the TSO/DSO boundary node operating points,” *Computers and Operations Research*, 2017.
- [22] CIGRE Task Force C6.04.02, „Benchmark Systems for Network Integration of Renewable and Distributed Energy Resources,” 2011.
- [23] Verband der Elektrotechnik Elektronik Informationstechnik e.V. (VDE), „VDE-AR-N 4105:2011-08: Power generation systems connected to the low-voltage distribution network,” VDE, 2011.
- [24] R. J. W. de Groot, J. Morren en J. G. Slootweg, „Investigation of Grid Loss Reduction under Closed-Ring Operation of MV Distribution Grids,” in *PES General Meeting*, National Harbor, MD, USA, 2014.